Eur. Phys. J. D (2015) 69: 8
DOI: 10.1140/epjd/e2014-50240-2

THE EUROPEAN PHYSICAL JOURNAL D

Regular Article

Bicoherence analysis of streamer dynamics induced by trapped ion modes*

Francesco Palermo[1,2,a], Xavier Garbet[2], and Alain Ghizzo[3]

[1] LMFA, École Centrale de Lyon, Université de Lyon, 69134 Ecully, France
[2] CEA, IRFM, 13108 Saint-Paul-Lez-Durance, France
[3] Institut Jean Lamour-UMR 7168, Université de la Lorraine, 54506 Nancy, France

Received 25 March 2014 / Received in final form 25 August 2014
Published online 8 January 2015 – © EDP Sciences, Società Italiana di Fisica, Springer-Verlag 2015

Abstract. High order spectral analyses have recently attracted a great deal of attention in the context of experimental studies for magnetic fusion. Among these techniques, bicoherence analysis plays an important role as it allows distinguishing between spontaneously excited waves and waves that arise from a coupling between different modes linked to specific physical mechanisms. Here, we describe and apply bicoherence analysis to kinetic simulations performed with reduced "bounce-averaged gyrokinetic" code, in order to investigate the nonlinear dynamics of trapped ion modes. This analysis shows a nonlinear wave coupling process linked to the formation of convective cells, thus furthers our understanding of the nonlinear energy transfer between turbulence structures in tokamaks.

1 Introduction

Cross-field transport of energy and particles in magnetically confined plasmas represents a major issue for achieving magnetic fusion. This transport is commonly attributed to small-scale turbulence generated by microinstabilities which are driven by temperature and density gradients along the radial direction in a tokamak. In particular, ion temperature-gradient driven modes, trapped electron modes and electron temperature-gradient driven modes are considered as the most important microinstabilities responsible for turbulent transport in magnetised plasmas with low $\beta = 2\mu_0 P/B^2$ values (where P is the plasma pressure and B is the magnetic field). The use of simulation code that accounts for kinetic effects is essential for studying turbulent transport. In fact, although a fluid treatment can give a first description, the nonlinear dynamics linked to these phenomena can be strongly affected by specifically kinetic mechanisms such as Landau Damping, finite orbit (FOW) effects and finite Larmor radius (FLR) effects. In general such kinetic code has to account for six-dimensions (6D), with 3 coordinates for positions, and 3 others for velocities. The disparate spatio-temporal length scales that are involved in tokamak turbulence lead to costly simulations. Hence several kinetic codes with reduced dimensionality have been developed, usually by eliminating high-frequency phenomena. Gyrokinetic codes are based on averaging the fast cyclotron time scale of particles and are now commonly used [1]. This operation, licit when the frequency of fluctuations is smaller than cyclotron frequencies, is well justified in most fusion devices. A further reduction step can be taken when instabilities are driven by particles that are trapped in the minima of the magnetic field. If the frequencies of modes are low enough, the dynamics can be averaged over the particle bounce motion along the field lines. These numerical tools are called "bounce-averaged gyrokinetic" codes. Reduced kinetic codes have strongly contributed to the understanding of physics of turbulent transport in slab and toroidal geometries. Regarding the dynamics of turbulent transport driven by temperature gradient instabilities, gyrokinetic simulations and experiments have shown the formation of structures which play an important role in turbulence self-organisation. The most well-known structures are zonal flows that are generated by fluctuations of turbulence and back-react via vortex shearing, thus reducing transport. Zonal flows can be identified by means of a perturbed electric field with wave vector $\boldsymbol{k} \approx (k_r, 0, 0)$ pointing in the radial direction. Structures called "streamers" are a counterpart of zonal flows. Streamers are convective cells which are elongated in the radial direction and offer an efficient channel for energy transport. As such they play an important role in turbulence self-organisation [2]. It is important to note that streamers are commonly observed in simulations but no clear evidence of their existence has been found in fluctuation measurements. Although there is a general consensus on their existence, the precise nature of

* Contribution to the Topical Issue "Theory and Applications of the Vlasov Equation", edited by Francesco Pegoraro, Francesco Califano, Giovanni Manfredi and Philip J. Morrison.

[a] e-mail: francesco.palermo@ec-lyon.fr

streamers is still being discussed. As indicated by Holland and Diamond [2] two distinct groups can be identified: "isolated intermittent streamers", which are caused by the nonlinear dynamics, and "streamer arrays", which are generated from linear and nonlinear processes. Streamers can thus be identified as perturbations rapidly changing in the poloidal direction but almost constant in the radial direction $\boldsymbol{k} \approx (0, k_\theta, 0)$. Streamers have been studied intensively because of their scientific impact, and because of their implications in Ion Temperature Gradient (ITG) turbulence and also as a channel of transport for Electron Temperature Gradient turbulence. Although these convective structures have been addressed in an extensive overview [3], some important aspects of their formation and interaction still need to be clarified. Consequently new methods of analysis become necessary to investigate them. *High order spectral analyses* have recently attracted a great deal of attention in the context of experimental studies for magnetic fusion [4–7]. The most popular spectral analysis tool is probably the bicoherence method, which was proposed by Kim and Powers [8]. Bicoherence allows one to investigate the degree of phase correlation among three waves and is related to the quadratic nonlinearities. It sheds light on the exchange of energy between modes that is due to specific physical mechanisms. This paper presents results from a bicoherence analysis tool that has been developed on the basis of the computational procedure developed by Kim and Powers. The objective is to elucidate the energy transfer mechanisms in the dynamics of turbulence, and to identify the structures that play a key role in kinetic simulations. Here we applied this analysis to simulations performed with a bounce-averaged gyrokinetic code that is specifically designed for studying low frequency instabilities driven by trapped ion (TIM). In toroidal geometry, the specific dynamics of TIM becomes important when the frequency of ITG modes falls below the ion bounce frequency, allowing one to average on both the cyclotron and bounce motion fast time scales. This reduction of the number of degrees of freedom leads to a strong reduction of the requested computer resources (memory and computation time). Therefore, long simulation runs compared to the ones that could be obtained with 5D gyrokinetic codes can be performed, while keeping the essential physical ingredients. In our model we have focused the analysis on the large scale dynamics of interchange-like instabilities to assess the nonlinear evolution of convective cells. We show and discuss results obtained by using a bicoherence analysis. The present article is organised as follows. In Section 2 we briefly recall the set of equations integrated in the bounce-averaged gyrokinetic code. In Section 3 we summarise the characteristics of the bicoherence analysis tool. In Section 4 we present and discuss results on three-wave coupling modes observed in the simulations. Finally, conclusions follow in Section 5.

2 Numerical model

The present model describes the dynamics of TIM modes, which are mainly driven by the gradient of temperature. The derivation of the equations and their implementation in TIM code have been discussed in previous works [9–11]. Hence only the main expressions are summarised and discussed. We consider an axi-symmetric toroidal geometry, with a magnetic axis located at a major radius R_0. The modulus of the magnetic field is $B(R_0 + r, \theta) \approx B_0[1 + \epsilon \sin^2(\theta/2)]$ in which $\epsilon = r/R_0$ is the inverse of the aspect ratio and B_0 is the minimum magnetic field at the angle $\theta = 0$. The motion of the particle can be separated into a fast cyclotron motion, with a time scale ω_c^{-1}, and a slower "gyrocenter motion". The analysis of the gyrocenter trajectories allows one to identify two different classes of particles called "passing particles" and "trapped particles", respectively. Circulating particles have a large enough parallel velocity to move on a magnetic field line on its entire length. Trapped particles follow a bouncing motion on the low field side, thus describing a "banana" orbit shape with a width δ_b in the radial direction. The trapped particle motion is characterised by a bounce frequency ω_b and a slower magnetic drift around the torus with a frequency ω_d [12]. Deeply trapped particles spend most of their time in the "bad" curvature zone of the tokamak, that is the zone where interchange-like modes are locally unstable. This aspect emphasises their possible role in turbulent transport. In collisionless plasmas, these instabilities are energised via Landau resonances between particles and waves in a range of frequencies that is well below the parallel transit frequency. This feature allows us to decouple the dynamics of trapped ions from passing ions. The density response of passing ions is then simply adiabatic. The existence of three motion invariants in the unperturbed case ensures that the system is integrable. These invariants are the magnetic momentum μ (also known as the adiabatic invariant), proportional to the magnetic flux across a cyclotron orbit, the particle energy E, and the toroidal canonical momentum M_k, which for a trapped particle coincides with the flux of the poloidal magnetic field ψ. Moreover the quasi-periodicity allows the construction of a set of action angle variables which are canonically conjugated (J_k, α_k) (with $k = 1, 2, 3$). This set of coordinates is well adapted to describe the motion of particles and implement the gyro- and bounce-averaging procedures. The system at equilibrium can be described by an unperturbed Hamiltonian $H = H_0(J_k)$ that is a function of the actions only, with J_1, J_2, J_3 related to the three invariants (μ, E, ψ). By means of the motion equations, the angle variables $\alpha_1, \alpha_2, \alpha_3$ are related respectively to the cyclotron ω_c, bounce ω_b and precession ω_d frequencies. The low frequency response for TIM is obtained by making a phase-angle average over the cyclotron and bounce motions (i.e. over the angles α_1 and α_2). Only the precession motion is explicitly taken into account in the model. Finally the two important variables are the precession phase α_3 (hereafter indicated by α) that is a function of toroidal and poloidal coordinates, and the poloidal flux ψ related to J_3 which plays the role of a radial coordinate.

These directions define a plane (α, ψ) that is orthogonal to the magnetic field. The code evolves a bounce-averaged distribution function $\bar{f}(\alpha, \psi)$ by solving a Vlasov

equation

$$\frac{\partial \bar{f}}{\partial t} + [\bar{\phi}, \bar{f}] + E\omega_d \frac{\partial}{\partial \alpha} \bar{f} = 0 \quad (1)$$

where $[.,.]$ is the usual Poisson Bracket $[g, f] = \partial_\psi g \partial_\alpha f - \partial_\alpha g \partial_\psi f$ and $\bar{\phi}$ is the bounce-averaged electric potential. In this expression the last term represents the interchange term that drives the main instability. Trapped ion turbulence develops on length scales of the order of the banana orbit width δ_b which is much larger than the Debye length. In this case, self-consistency is ensured by the quasi-neutrality condition, instead of the Poisson equation. Thus assuming an adiabatic response for electrons, the electro-neutrality condition is written as:

$$C_e \left(\phi - \langle \phi \rangle_\alpha\right) = C_i \overline{\nabla}^2 \phi + \bar{n}_i - n_0 \quad (2)$$

where the left hand side indicates that the electron density vanishes when the electric potential equals its flux average $\langle \phi \rangle_\alpha$. The latter represents the potential averaged on a magnetic surface (constant ψ surface) by means of the operator $\langle . \rangle_\alpha$. In equation (2), n_0 is the total ion density and $\bar{n}_i$ represents the ion guiding centre density obtained by integrating the distribution function on the velocity space expressed in action-angle variables. The polarisation $\overline{\nabla}^2 \phi$ term is an approximation of the difference of particle and guiding centre densities. $C_e = (1+\tau)/f_p$ and $C_i = C_e f_p/\tau$ are constants accounting for the ratio τ of ion to electron temperatures, and for the fraction of trapped particles $f_p = 2\sqrt{2\varepsilon}/\pi$ which is mainly determined by the inverse aspect ratio ε. Finally, we note that the electron polarisation can be neglected because of their small mass. In summary, our kinetic trapped-ion model is given by a reduced Vlasov equation, self-consistently coupled to the electric potential ϕ. In the code, the time t is normalised to the inverse drift frequency $\omega_{d,0}^{-1}$ of reference, the poloidal flux ψ is counted in $\Delta\psi = \pi r_0^2 B_0/q$ units, the energy E is normalised to a temperature T_0, and the potential ϕ is given in $\omega_{d,0}\Delta\psi$ units.

3 Bicoherence analysis

As mentioned in the introduction, bicoherence represents a useful tool to investigate the nonlinear dynamics, as it allows one to distinguish between spontaneously excited waves and coupled waves in a fluctuation spectrum. This information is not contained in the energy spectra of a signal based on the linear analysis of the Fourier decomposition such as the power spectrum $P(k) = |X_k|^2$ (with X_k k-fourier coefficient). In a signal, nonlinear wave-wave interaction can be observed when the conditions $k_3 = k_1 + k_2$ ($f_3 = f_1 + f_2$) and $\varphi_3 = \varphi_1 + \varphi_2$ are satisfied between three waves with wavenumbers k_1, k_2, k_3 (or frequencies f_1, f_2, f_3) and phases φ_1, φ_2, φ_3. In the case where φ_3 behaves in a random way, the associated wave evolution is not linked to other two waves. In summary, the bicoherence measures the degree of coherence of the three wave phases. It is quantified by the following expression:

$$b(k,l) = \frac{|\frac{1}{M}\sum_{j=1}^{M} X_k^{(j)} X_l^{(j)} X_{k+l}^{*(j)}|}{[\frac{1}{M}\sum_{j=1}^{M} |X_k^{(j)} X_l^{(j)}|^2]^{1/2} [\frac{1}{M}\sum_{j=1}^{M} |X_{k+l}^{(i)}|^2]^{1/2}}, \quad (3)$$

where M represents the number of independent data records of a signal. It is not straightforward to calculate the bicoherence because of the variability of the denominator that can produces spurious spikes in the associated spectrum [8,13]. However, neglecting the variability of the denominator, Kim and Powers [8] have shown that the variance, which measures the degree of accuracy of the squared bicoherence, can be approximated by the expression $\mathrm{var}(b^2) \approx (1 - b^2)1/M$. We note that $\mathrm{var}(b^2) \leqslant 1/M$ and consequently the variance approaches 0 as M becomes infinite. The numerator of equation (3) is known as the bispectrum. Bicoherence is thus a normalised bispectrum that varies between 1 (for a three wave coherence relation) and 0 (corresponding to no-coherence phase relation). Bicoherence can be represented graphically in the (k,l)-plane by the inner triangular region defined by $0 \leq l \leq a/2$ and $l \leq k \leq (a - l)$ where $a = k_N/\Delta k$ with k_N Nyquist limit number and $\Delta k = 1/T$ bandwidth of the signal. Indeed, for a single regular signal it is sufficient to compute the bicoherence over this region because the information is redundant in all the other regions of the plane. In the case where bicoherence is calculated between multiple quantities, the non-redundant information region has the shape of a peculiar polygonal domain. Taking as reference the work of Kim and Powers [8], we have developed a bicoherence tool on the basis of equation (3). For the sake of discussion, we show an application of this tool on the following signal:

$$g(x) = R(x) + \cos(k_1 x + \varphi_1) + \cos(k_2 x + \varphi_2) + \cos(k_1 x + \varphi_1)\cos(k_2 x + \varphi_2) \quad (4)$$

with $k_1 = 0.22 k_N$, $k_2 = 0.37 k_N$ and where $R(x)$ is a random signal. The last term in equation (4) generates two signals of type $0.5\cos(k_\pm x + \varphi_\pm)$ with $k_\pm = k_1 \pm k_2$ corresponding to the sum and the difference of original wavenumbers k_1, k_2 and $\varphi_\pm = \varphi_2 \pm \varphi_1$. Squared bicoherence in Figure 1 shows two peaks at the points $[k_2, k_1]$ and $[k_1, k_-]$ and the background noise is evident in the triangular spectrum domain. The relationship of the phase between the components of the signal in equation (4) are summarised in Table 1. We note that the bicoherence analysis can only confirm the existence of mode coupling between three waves, but cannot determine the causal relationship between the waves or which wave is generated by the other two waves.

4 Results and discussion

In this section, we applied a bicoherence analysis to a simulation performed with a bounce-averaged gyrokinetic code in order to investigate the nonlinear dynamics of TIM instabilities. We recall that the most important feature of

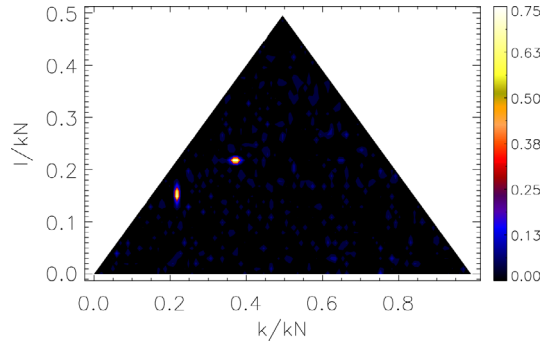


Fig. 1. Squared bicoherence spectrum corresponding to signal of equation (4).

Table 1. Frequency relation for the signal in equation (4). Considering phase relations, two peaks are expected in the bicoherence spectrum.

	k relations	Phase relations	Peak locations
1	$k_1 + k_2 = k_+$	$\varphi_1 + \varphi_2 = \varphi_+$	$[k_2, k_1]$
2	$k_1 + k_- = k_2$	$\varphi_1 + \varphi_- = \varphi_2$	$[k_1, k_-]$

the TIM model is that high-frequency phenomena such as the cyclotron motion and the bounce motion of trapped ions have been eliminated, while essential kinetic effects for low frequency instabilities are kept. Modes such as TIM are a prototype of kinetic instability since they are driven through the resonant interaction between waves and trapped ions via the toroidal precession of banana orbits. The starting point for the investigation of TIM instability is the gyrokinetic Vlasov model coupled to the quasi-neutrality condition initiated in an equilibrium state with a perturbed term. The initial distribution function and electrostatic potential perturbations are as follows:

$$\bar{f}\,(\alpha,\psi) = \bar{F}_0\,(\psi) + \sum_{k_\alpha} \delta\bar{f}_{k_\alpha}\,(\psi)\, e^{i(k_\alpha \alpha)} \tag{5}$$

$$\phi = \phi_0\,(\psi) + \sum_{k_\alpha} \delta\phi_{k_\alpha}\,(\psi)\, e^{i(k_\alpha \alpha)} \tag{6}$$

where $\delta\phi_{k_\alpha}(\psi) = \sin(n\pi\psi)$ with $n = 1$. The $\bar{F}_0(\psi)$ and $\phi_0(\psi)$ equilibrium functions are equal to:

$$F_0\,(\psi) = e^{-E}\left[1 + \Delta\tau_s\omega_d\left(E - \frac{3}{2}\right)\psi\right] \tag{7}$$

$$\phi_0\,(\psi) = 0 \tag{8}$$

where $\Delta\tau_s$ is normalised temperature gradient. TIM instabilities are driven by the temperature gradient with the possibility of a resonance arising between trapped waves and ions through their precession motion. Density $N\,(\psi)$ and temperature profile $T\,(\psi)$ can be obtained as fluid momenta of the distribution function $\bar{F}_0$. In this way, we obtain an almost flat profile of density $N = 1$ and the following profile of temperature:

$$T\,(\psi) = 1.5\,(1 + \Delta\tau_s\psi\;\omega_d) \tag{9}$$

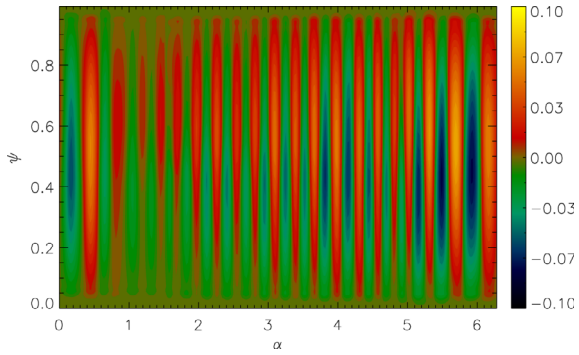


Fig. 2. Isocontours of potential at $t = 15.5$ showing formation of about 22 streamer structures.

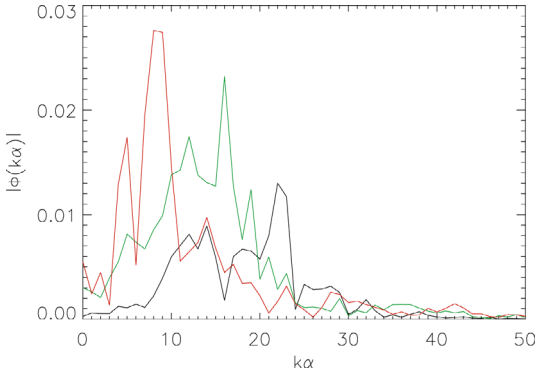


Fig. 3. k_α spectrum plot at $t = 15.5$ (black line), 19.5 (green line), 35 (red line).

with $\omega_d = 0.9$. We have considered $n_\psi \times n_\alpha = 128 \times 256$ phase space sampling. We have chosen an ion-electron temperature ratio $\tau = 1$ and we have used the following parameter values: $C_e = 0.61$, $C_i = 0.5$; the time step is $\Delta t = 0.005$ and the initial perturbed potential amplitude is $\delta\phi \sim 10^{-5}$. The ion banana orbit width $\delta_b = 0.09$ is three times the Larmor radius. With the selected C_e and δ_b values, the stability threshold temperature is $\Delta\tau_0(C_e, \delta_b) = 0.6$ (for detail see Ghizzo et al. [11]). The value $\Delta\tau_s = 0.8$ has been chosen in equation (9) in order to get a sufficient drive. It is interesting to consider the behaviour of the system in the first phase of the dynamics, when TIM modes are dominant. In Figure 2 we show the isocontour of the potential perturbations in the (α, ψ)-box and we observe nonlinear streamers formation in the first phase at $t = 15.5$. These structures appear in the simulation as an effect of the TIM instability that provides evidence for the dominance of interchange modes along the ψ direction. The formation of streamers is well identified also in the spectrum performed along the α direction. In Figure 3 we show the principal modes that grow in the simulation at three different times $t = 15.5$ (black line), 19.5 (green line), and 35.0 (red line). The energy is initially injected in the system in the range $10 \lesssim k_\alpha \lesssim 15$. At time $t = 15.5$ we observe that the modes around $k_{\alpha,S} \approx 22$ become dominant. In order to investigate the onset of modes we perform a bicoherence analysis in the plane (ψ, α). For this purpose we consider

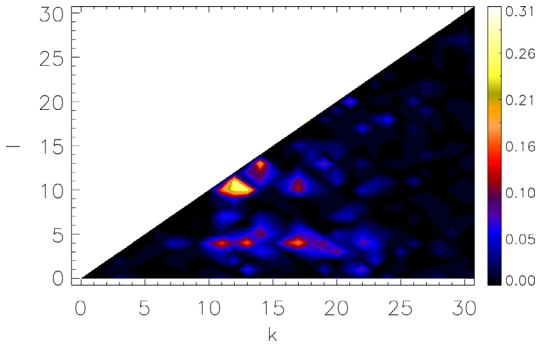


Fig. 4. Zoom of squared bicoherence spectrum on the first 30 modes at $t = 15.5$.

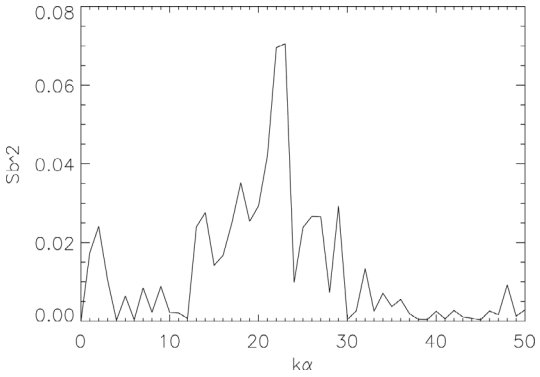


Fig. 5. "Summed bicoherence" spectrum $0 \leq k_\alpha \leq 50$ at $t = 15.5$.

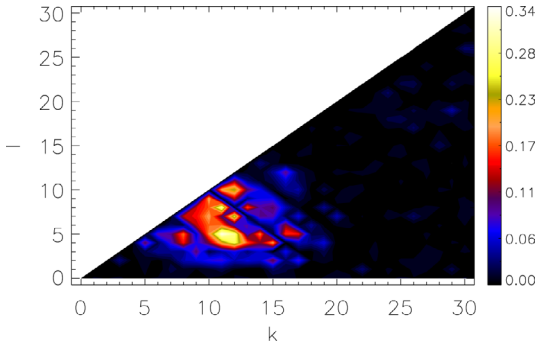


Fig. 6. Zoom of squared bicoherence spectrum on the first 30 modes at $t = 19$.

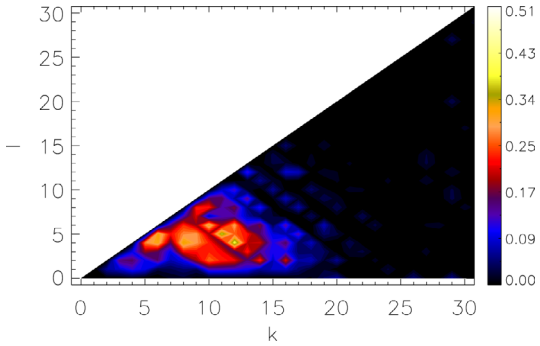


Fig. 7. Zoom of squared bicoherence spectrum on the first 30 modes at $t = 21$.

profiles of the potential between $\psi_1 = 0.2$ and $\psi_2 = 0.8$ along the α direction. These profiles correspond to data records of the signal. Considering $M = 80$ profiles we find $var(b^2) \leqslant 0.01$. In Figure 4 the squared bicoherence analysis performed at $t = 15.5$ shows a significant bicoherence value ($b^2 \approx 0.31$) for modes $(k, l) \approx (12, 10)$. In order to interpret this signal, it is useful to calculate a "summed bicoherence" defined as $Sb^2(k_\alpha) = 1/s \sum b^2(k, l)$ where the sum is taken over all k and l such as $k + l = k_\alpha$ and where s is the number of terms in the sum for a given value of k_α. Figure 5 shows this summed bicoherence. A peak is observed around $k_{\alpha,S} \approx 22$. Then, a strong coupling appears, of the type $k + l = k_\alpha$ for modes $(12 + 10) \approx (11 + 11) \approx 22$. We emphasise that a bicoherence analysis can only confirm the existence of mode coupling between three waves, but cannot determine the causal relationship between the modes or which mode is generated by the other two modes. For this purpose, several methods have been proposed to determine the direction of energy transfer [6,14]. Here we use the profile of the spectrum at different times to estimate this transfer direction. When doing so, the bicoherence shows which modes are involved in the nonlinear coupling and the temporal evolution of the spectrum provides an information on the chronology and the direction of the energy transfer between these modes. Streamers can be identified as the first harmonic of modes around $k_{\alpha,F} \approx 11$ that develop in the system. In Figure 6 we show the squared bicoherence spectrum calculated at $t = 19$. We observe again the coupling of harmonics $k_{\alpha,S} \approx 2\, k_{\alpha,F}$ and at the same time we observe the development of a strong interaction between different (k, l) modes whose sum is equal to $k_{\alpha,S} \approx 22$ such as $(k + l) \approx (12 + 10) \approx (15 + 7) \approx (17 + 5)$. Comparing the spectral profile at $t = 15, 5$ and $t = 19$ in Figure 3, we deduce that the energy initially transferred on the specific mode $k_{\alpha,S} \approx 22$ is distributed on different lower modes by means of nonlinear coupling interaction. These new modes interact between themselves, and in particular the mode $k_{\alpha,I} = 16$ is generated by nonlinear interaction, as shown by the spectral profile and the squared bicoherence at $t = 19$ in which we observe an important peak ($b^2 \approx 0.34$) around $(k, l) \approx (11, 5)$. After a growing phase, the $k_{\alpha,I} = 16$ mode saturates and releases its energy on lower k_α modes. A second nonlinear energy transfer, similar to that of $k_{\alpha,S} = 22$, is found for $k_{\alpha,I} = 16$ in the bispectrum at $t = 21$ shown in Figure 7, in which we observe the coupling of different modes whose sum is equal to $k_{\alpha,I} = 16$ such as $(k+l) \approx (12+4) \approx (13+3) \approx (14+2)$. At the same time, we observe an interaction of modes localised between $5 \lesssim k \lesssim 10$ for $l \approx 5$. The spectrum shown in Figure 3 indicates that lower modes are amplified at $t = 35$, in particular the modes $k_\alpha \approx 5, 8$. The nonlinear mechanism that determines this sequential inverse energy cascade can be qualitatively found in Figure 8, in which isocontours of potential are shown at $t = 39$. In this figure we observe the interaction of streamers characterised by nonlinear merging, which are able to generate more and more low wavenumber modes along the poloidal direction. At the same time, we can identify k_ψ modes that develop

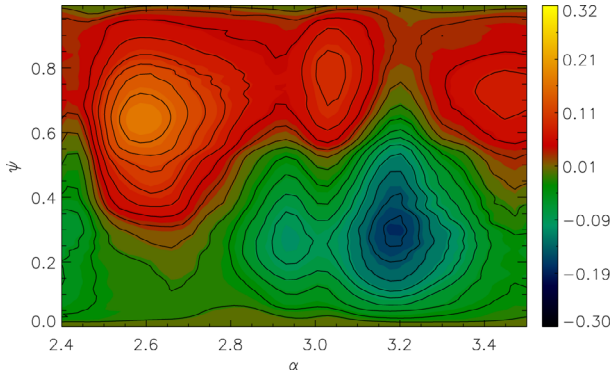


Fig. 8. Isocontours of potential at $t = 39$ in the region $2.4 \leq \alpha \leq 3.5$.

along the radial direction. This observation has important implications for zonal flows formation and their interaction with streamers. The detailed mechanism of streamer interactions and zonal flow formation will be the subject of a future work (in preparation). Here we would like to emphasise the dynamics of streamers. We have observed that energy is injected in the system via selected modes that determine the size of streamers. These structures saturate after a growing phase. By means of a bicoherence analysis we demonstrated that a large fraction of their energy is released on scales larger than the initial one. So new localised modes, at large scale, increase in time and subsequently saturate by transferring in turn their energy on larger scales. This process defines an interesting intermittent inverse energy cascade.

5 Conclusions

In this paper we have described and applied a bicoherence analysis to simulations performed with a bounce-averaged gyrokinetic code that can be considered as a toy model that is able to describe the basic structures of turbulent transport in tokamaks such as streamers and zonal flows. The advantage of this code is the possibility to investigate the dynamics of these structures on longer times, compared to those that could be reached with full 5D gyrokinetic codes. We emphasise that understanding the dynamics of streamers and zonal flows is a quite important problem, since the confinement in a tokamak depends on the respective level and life time of these structures. With our code, we have observed the development of TIM instabilities through the formation of streamer structures. This instability is akin to a Rayleigh-Benard instability and is able to transport large quantities of energy towards the exterior zone of tokamak, by means of a convective transport mode regulated by streamers. Here, we have shown that streamers can saturate by transferring energy to large scale structures. In particular, by using a bicoherence analysis tool and analysing the time evolution of the spectral profile, we have shown that the transfer of energy is due in large part to a nonlinear coupling of modes along the α direction. Thus, most of the energy initially injected on modes that determine the size of streamers is transferred on lower modes via an intermittent mechanism of inverse energy cascade. Consequently, the transport of energy along the ψ direction is affected. Moreover, we have observed that at the same time k_ψ modes develop along the radial ψ direction. This has potential implications on the interaction between zonal flows and streamers that are involved in the generation of zonal flows. This aspect could be very relevant for the control of turbulence suppression and consequently for the development of magnetic fusion.

This work has been supported by French National Research Agency under contract ANR GYPSI, ANR-10 Blanc-941, SIMI9 2010.

References

1. X. Garbet et al., Nucl. Fusion **50**, 043002 (2010)
2. C. Holland, P.H. Diamond, Phys. Lett. A **344**, 369 (2005)
3. P.H. Diamond et al., Plasma Phys. Control. Fusion **47**, R35 (2005)
4. B.Ph. van Milligen et al., Nucl. Fusion **52**, 013006 (2012)
5. M. Xu et al., Phys. Plasmas **16**, 042312 (2009)
6. T. Yamada et al., Phys. Plasmas **17**, 052313 (2010)
7. D.F. Kong et al., Nucl. Fusion **53**, 113008 (2013)
8. Y.C. Kim, J. Powers, IEEE Trans. Plasma Sci. **7**, 120 (1979)
9. G. Depret et al., Plasma Phys. Control. Fusion **42**, 949 (2000)
10. Y. Sarazin et al., Plasma Phys. Control. Fusion **47**, 1817 (2005)
11. A. Ghizzo et al., Phys. Plasmas **17**, 092501 (2010)
12. B.B. Kadomtsev, O.P. Pogutse, Nucl. Fusion **11**, 67 (1971)
13. B.Ph. van Milligen et al., Phys. Plasmas **2**, 3017 (1995)
14. B.Ph. van Milligen et al., Nucl. Fusion **17**, 023011 (2014)